Math. Model. Nat. Phenom.
Vol. 11, No. 2, 2016, pp. 44–62
DOI: 10.1051/mmnp/201611204

Eigenfunction Approach to Transient Patterns in a Model of Chemotaxis

P. Chatterjee[1], B. Kazmierczak[1] *
[1] Institute of Fundamental Technological Research Polish Academy of Sciences

Abstract. In the paper we examine solutions to a model of cell movement governed by the chemotaxis phenomenon derived in [14] and established via macroscopic limits of corresponding microscopic cell-based models with extended cell representations. The model is given by two PDEs for the density of cells and the concentration of a chemical. To avoid singularities in cell density, the aggregating force of chemotaxis phenomenon is attenuated by a density dependent diffusion of cells, which grows to infinity with density tending to a certain critical value. In this paper we recover the quasi-periodic structures provided by this model by means of (local in time) expansion of the solution into a basis of eigenfunctions of the linearized system. Both planar and spherical geometries are considered.

Keywords and phrases: pattern formation, chemotaxis, Turing bifurcation, eigenfunction expansion

Mathematics Subject Classification: 35B36, 35B20, 35B32, 65N25, 65P30

1. Introduction

In [14], a model of cell motility due to diffusion and chemotaxis phenomenon was derived via macroscopic limit of appropriate microscopic system describing stochastic motion of cells. This macroscopic model is governed by two partial differential equations of cell density and chemical concentration. In this model, nonlinear diffusion equation is derived from microscopic dynamics, and the diffusion coefficient, preventing collapse of cellular density, depends on cellular volume fraction.

*Corresponding author. E-mail: bkazmier@ippt.pan.pl

The nonlinear spatially two-dimensional diffusion equation for the evolution of cellular density $p(\mathbf{r},t)$ proposed in [14] has the form:

$$\partial_t p(\mathbf{r},t) = D\nabla_{\mathbf{r}} \cdot (\Gamma(\phi)\nabla_{\mathbf{r}} p(\mathbf{r},t)) - \chi_0 \nabla_{\mathbf{r}} \cdot [p(\mathbf{r},t)\nabla_{\mathbf{r}} c(\mathbf{r},t)] \tag{1.1}$$

where $\mathbf{r} = (x,y)$ is a vector of spatial coordinates and

$$\Gamma(\phi) = \frac{1+\phi}{1-\phi+\phi \ln(\phi)}\,. \tag{1.2}$$

This nonlinear diffusion equation is coupled with equation for the evolution of the chemical field $c(\mathbf{r},t)$:

$$\partial_t c(\mathbf{r},t) = D_c \nabla^2_{\mathbf{r}} c(\mathbf{r},t) + \tilde{a} p(\mathbf{r},t) - \gamma c(\mathbf{r},t). \tag{1.3}$$

In equation (1.1), ϕ is the local volume fraction occupied by cells. It is assumed that cells are fluctuating rectangles and $\phi = L_x^{(0)} L_y^{(0)} p(\mathbf{r},t)$, where $L_x^{(0)}, L_y^{(0)}$ are average length and width of a cell. Thus system (1.1) and (1.3) can be written in an equivalent way:

$$\partial_t \phi(\mathbf{r},t) = D\nabla_{\mathbf{r}} \cdot (\Gamma(\phi(\mathbf{r},t))\nabla_{\mathbf{r}} \phi(\mathbf{r},t)) - \chi_0 \nabla_{\mathbf{r}} \cdot [\phi(\mathbf{r},t)\nabla_{\mathbf{r}} c(\mathbf{r},t)], \tag{1.4}$$

$$\partial_t c(\mathbf{r},t) = D_c \nabla^2_{\mathbf{r}} c(\mathbf{r},t) + a\phi(\mathbf{r},t) - \gamma c(\mathbf{r},t) \tag{1.5}$$

where

$$a = \frac{\tilde{a}}{L_x^{(0)} L_y^{(0)}}\,. \tag{1.6}$$

Equations (1.4)-(1.5) are considered in a set $\Omega \times (0,T)$, where $\Omega \subset \mathbb{R}^2$ and $T > 0$. It is supplemented by the no-flux boundary conditions

$$\frac{\partial \phi}{\partial n}(\mathbf{r},t) = 0, \quad \frac{\partial c}{\partial n}(\mathbf{r},t) = 0 \quad \text{for } (\mathbf{r},t) \in \partial\Omega \times (0,T) \tag{1.7}$$

where $\partial\Omega$ is the boundary of the domain Ω and n is the unit outward normal to $\partial\Omega$. Initial conditions are

$$\phi(\mathbf{r},0) = \phi_0(\mathbf{r}), \quad c(\mathbf{r},0) = c_0(\mathbf{r}). \tag{1.8}$$

In equation (1.4), D is the diffusion coefficient for a motion of an isolated cell, χ_0 defines strength of chemotactic interactions with

$$\chi_0 = D\ \mu\beta L_x^{(0)} L_y^{(0)} \tag{1.9}$$

where $(-\mu)$ is an effective chemical potential, $\beta = 1/T$ is the inverse effective temperature T of the cellular shape fluctuations, and

$$L_x^{(0)} = L_{T_x} - J_{cm}/\lambda_x,\ L_y^{(0)} = L_{T_y} - J_{cm}/\lambda_y. \tag{1.10}$$

$L_{T_{x(y)}}$ are the target values of $L^{(0)}_{x(y)}$ and λ_x, λ_y are suitable Lagrange multipliers. J_{cm} is the binding energy per unit length (see [14]).

In equation (1.5), D_c is the diffusion coefficient of the chemical c, $\tilde{a}$ is its production rate, and γ is the decay rate.

The global in time existence of solutions to this system and some of their properties have been considered in [1].

System (1.4)-(1.5) can be used for description of biological phenomena, like formation of open network structures in limb cell cultures [5,6] and vasculogenesis [9,10], where a population of cells interact directly and via diffusible factors. These processes are crucial in embryo development. Aggregating mechanisms in limb cells lead to the formation of chondrogenetic structures, whereas vasculogenesis leads to the formation of blood vessels in the embryo. In [14], examples of applications of system (1.4)-(1.5) were analyzed numerically. In particular, an interim pattern for relatively small times has been obtained numerically starting from random initial data (see Figure 6 in [14]). Such patterns may be transient as a solution to system (1.4)-(1.5), i.e. it may exist for some time and then disappear, or it may be unstable. However, in this paper we are not interested in the asymptotic behaviour of this local in time pattern. Such an approach may be justified by the fact that many biological systems pass through the weakly non-stable states (transient patterns), which can be stabilized by another kind of phenomenon (not taken into account in the considered model).

The specific aim of our study is to recover the quasi-periodic structures provided by the model (1.4)-(1.5) by using their expansion in terms of eigenfunctions of the linearized system. The symbolic program in Mathematica is used for calculating such expansion. We will be interested both in the planar and in the spherical case. The spherical case may correspond to the process of angiogenesis on the surface of the tumour region. It may also refer to the process of receptor clusterization in the phenomenon of immune cell activation.

2. Absence of patterns for small values of μ

First, let us state a nonnegativity lemma. The nonnegativity of solutions to system (1.4)-(1.5) subject to nonnegative initial data follows from Theorem 1 in [1]. Here, for the reader's convenience, we will sketch an independent proof of this fact.

Lemma 2.1. *Suppose that ϕ and c are solutions to system (1.4)-(1.5) of class $C^{2,1}_{r,t}(\Omega\times(0,T))$. Suppose that $\phi_0(\boldsymbol{r})\geq 0$ and $c_0(\boldsymbol{r})\geq 0$ for all $\boldsymbol{r}\in\Omega$. Then $\phi(\boldsymbol{r},t)\geq 0$ and $c(\boldsymbol{r},t)\geq 0$ for all $(\boldsymbol{r},t)\in\Omega\times(0,T)$. Moreover,*

$$\frac{\partial}{\partial t}\int_\Omega \phi(\boldsymbol{r},t)d\boldsymbol{r}=0. \tag{2.1}$$

It means that the volume fraction occupied by cells is conserved in the course of evolution.

Proof. To prove the positivity let us first extend the function Γ for $\phi<0$ in the space of continuous functions by assuming that $\Gamma(\phi)\equiv\Gamma(0)=1$ and the derivative of $\Gamma(\phi)$ is continuous. Now, we

may proceed, e.g. using the method applied in [13] to a model having the similar structure but differing in the form of the nonlinear diffusion coefficient function. Next, integrating the both sides of equation (1.4) over the region Ω, applying Gauss-Ostrogradskii's theorem and using the zero-flux boundary conditions for ϕ and c we obtain (2.1). □

In our next step, we will prove that non-constant stationary solutions to system (1.4)-(1.5) exist only for sufficiently large chemotaxis constant χ_0. Thus let us consider the stationary counterpart of the system (1.4)-(1.5):

$$D\nabla_{\mathbf{r}} \cdot (\Gamma(\phi(\mathbf{r}))\nabla_{\mathbf{r}}\phi(\mathbf{r})) - \chi_0 \nabla_{\mathbf{r}} \cdot [\phi(\mathbf{r})\nabla_{\mathbf{r}} c(\mathbf{r})] = 0, \tag{2.2}$$

$$D_c \nabla^2_{\mathbf{r}} c(\mathbf{r}) + a\phi(\mathbf{r}) - \gamma c(\mathbf{r}) = 0. \tag{2.3}$$

Let $\chi_0 = 0$. Then expanding the diffusion term in the first equation and integrating over Ω, we obtain by means of the non-flux boundary conditions (1.8) that

$$D \int_{\Omega} \Gamma_{,\phi}(\phi(\mathbf{r}))\ (\nabla_{\mathbf{r}}\phi(\mathbf{r}))^2 d\mathbf{r} = 0.$$

Obviously, for $\phi \in (0,1)$ and $\Gamma(\phi)$ given by (1.2), $\Gamma_{,\phi}(\phi) > 0$. Hence Eq.(2.2) has no non-constant solutions with the values in the open interval $(0,1)$. Consequently, $\phi \equiv \phi_0 = const$. It follows that Eq.(2.3) can be written as

$$D_c \nabla^2_{\mathbf{r}} p(\mathbf{r}) - \gamma p(\mathbf{r}) = 0$$

where $p(\mathbf{r}) = c(\mathbf{r}) - a\gamma^{-1}\phi_0$. Multiplying the last equation by $p(\mathbf{r})$ and integrating we conclude that $\int_\Omega [D_c(\nabla_{\mathbf{r}} p(\mathbf{r}))^2 + \gamma p(\mathbf{r})^2] d\Omega = 0$ implying that $p(\mathbf{r}) \equiv 0$ and consequently that $c(\mathbf{r}) \equiv a\gamma^{-1}\phi_0$.

We will prove that for $\chi_0 > 0$, but sufficiently small, system (2.2)-(2.3) has also only constant solutions. To do it, according to Lemma 2.1, we will supplement the system with conditions expressing the preservation of L^1-norm of the component ϕ. That is to say, we demand that

$$\int_{\Omega} \phi(\mathbf{r}) d\mathbf{r} = \phi_0 |\Omega|. \tag{2.4}$$

Lemma 2.2. *For all $0 < \chi_0 < k_0$ with some $k_0 > 0$ sufficiently small, the only solution to system (2.2),(2.3),(2.4) is equal to a spatially homogeneous solution $(\phi, c) \equiv (\phi_0, a\gamma^{-1}\phi_0)$.*

Proof. To evade technical difficulties we will make a simplifying assumption that Ω has a smooth boundary of $C^{2+\alpha}$ class with $\alpha \in (0,1)$. The case of $\partial\Omega$ having a finite number of singular points (like a rectangle defined in (3.5) and considered in the sequel) can be treated similarly. We will use the implicit function theorem. If we decompose $\phi(x) = \psi(x) + \phi_0$. Then solutions to system (2.2),(2.3),(2.4) can be viewed as zeros of the mapping:

$$M : (\psi, c, \lambda) \rightarrow$$

$$\Big(D\nabla_{\mathbf{r}} \cdot (\Gamma(\psi(\mathbf{r}) + \phi_0)\nabla_{\mathbf{r}}\psi(\mathbf{r})) - \lambda^2\nabla_{\mathbf{r}} \cdot [(\psi + \phi_0)(\mathbf{r})\nabla_{\mathbf{r}}c(\mathbf{r})],$$

$$D_c\nabla^2_{\mathbf{r}}c(\mathbf{r}) + a(\psi + \phi_0)(\mathbf{r}) - \gamma c(\mathbf{r}), \int_\Omega \psi(\mathbf{r})d\mathbf{r}\Big).$$

This mapping acts from the space $(\psi, c, \lambda) \ni C^{2+\alpha}_N(\Omega) \times C^{2+\alpha}_N(\Omega) \times \mathbb{R}$ to the space $C^\alpha(\Omega) \times C^\alpha(\Omega) \times \mathbb{R}$. Here $C^{2+\alpha}_N(\Omega)$ denotes the Banach space of twice continuously differentiable functions in Ω with α-Hölder continuous second derivatives, satisfying the homogeneous Neumann boundary conditions (see (1.7)), with the usual 'sup' norm, $C^\alpha(\Omega)$ the Banach space of α-Hölder continuous functions with the 'sup' norm, and λ^2 stands for χ_0. The mapping is well defined in some vicinity of the point $(\phi, c, \lambda) = (\phi_0, a\gamma^{-1}\phi_0, 0)$. The Frechet derivative (with respect to (ψ, c)) $\mathcal{D}M_0$ at the point $(\phi_0, a\gamma^{-1}\phi_0, 0)$ of the mapping M acting on the increments $(\delta\psi, \delta c)$ has the form:

$$\mathcal{D}M_0(\delta\psi, \delta c) =$$

$$\Big(D\Gamma(\phi_0)\nabla^2_{\mathbf{r}}\delta\psi(\mathbf{r}), D_c\nabla^2_{\mathbf{r}}\delta c(\mathbf{r}) + a\delta\psi(\mathbf{r}) - \gamma\delta c(\mathbf{r}), \int_\Omega \delta\psi(\mathbf{r})d\mathbf{r}\Big).$$

This mapping is boundedly invertible. According to the theory of elliptic operators, to prove this fact, it suffices to show that the system

$$\mathcal{D}M_0(\delta\psi, \delta c) = (0, 0, 0)$$

has only zero solution. Thus multiplying the first equation $D\Gamma(\phi_0)\nabla^2\delta\psi(\mathbf{r}) = 0$ by $\delta\psi$ and integrating, we can conclude that $\int_\Omega(\nabla\psi)^2 d\Omega = 0$. Hence $\delta\psi \equiv const$ and the third equation implies that $\delta\psi \equiv 0$. Next, multiplying the second equation by c we obtain $\int_\Omega[D_c(\nabla_{\mathbf{r}}\delta c)^2 + \gamma(\delta c)^2]d\Omega = 0$, which implies that $\delta c \equiv 0$. Now, due to the implicit function theorem, the solution to system (2.2),(2.3),(2.4) can be obtained as a sequence of successive approximations and it is easy to prove that all the elements of this sequence are equal to zero. □

3. Eigenfunction expansion in the planar case

In this section we propose an approximate method of tracking the evolution of solutions of the system (1.4)-(1.5) via expansion of solutions on a basis of orthogonal functions in the region Ω. This set will be formed by the eigenfunctions corresponding to linearization of the operators at the right hand sides of equations (1.4)-(1.5). The linearization is done at an appropriately chosen spatially constant steady state corresponding to the chosen total number of cells. That is to say, for sufficiently small times we track the evolution of the initial data by means of the series composed of eigenfunctions corresponding to a spatially constant steady state with coefficients depending on the initial data and time.

Due to section 2, possible non-constant stationary patterns can exist only for sufficiently large values of the parameter χ_0. Moreover, to be observed experimentally (or numerically for very long time scales), these stationary solutions should be stable. In this paper we will be however be interested in transient patterns, i.e. patterns which are not necessarily stable as solutions to system (1.4)-(1.5), but may be an onset for patterns stabilized by some other factors not taken into account in the model of chemotaxis considered here. To be more precise, we are especially interested in the evolution of a random perturbation of the spatially homogeneous initial data. Principally our approach is to obtain spatial patterns follows the Turing bifurcation methodology. In the case of system (1.4)-(1.5), the constant steady states are not isolated, because they are of the form $(\phi, c) = (\phi_0, c_0) = (\phi_0, a\gamma^{-1}\phi_0)$ for any $\phi_0 > 0$, but due to Lemma 2.1 the L^1-norm of the initial data are conserved. To follow the path worked out by the Turing bifurcation theory, let us start from linearizing system (1.4) -(1.5) around the constant steady state (ϕ_0, c_0) and calculate the eigenvalues and eigenfunctions of the resulting system. The linearized time dependent system has the form

$$\partial_t \phi(\mathbf{r}, t) = D\Gamma(\phi_0)\nabla^2_{\mathbf{r}}\phi - \chi_0\phi_0\nabla^2_{\mathbf{r}}c, \tag{3.1}$$

$$\partial_t c(\mathbf{r}, t) = D_c\nabla^2_{\mathbf{r}}c + a\phi - \gamma c. \tag{3.2}$$

This system can be written as

$$\mathbf{u}_t = \mathbf{D}\nabla^2_{\mathbf{r}}\mathbf{u} + \mathbf{B}\mathbf{u} \tag{3.3}$$

where

$$\mathbf{u} = \begin{pmatrix}\phi\\ c\end{pmatrix}, \quad \mathbf{D} = \begin{bmatrix}D\Gamma(\phi_0) & -\chi_0\phi_0\\ 0 & D_c\end{bmatrix}, \quad \mathbf{B} = \begin{bmatrix}0 & 0\\ a & -\gamma\end{bmatrix}. \tag{3.4}$$

Before proceeding, let us specify the spatial region Ω, which we will consider in the planar case. We thus assume that for some $A > 0$

$$\Omega := \{(x, y) : 0 < x, y < A\}. \tag{3.5}$$

We will seek the solutions of system (3.3) as a linear combination of vector functions of the form

$$\mathbf{W} = \mathbf{E}\, cos(\frac{\pi kx}{A})\, cos(\frac{\pi ly}{A}) \tag{3.6}$$

where $k, l \in \mathbb{N} \cup \{0\}$ and $\mathbf{E} \in \mathbb{R}^2$ should be appropriately chosen. Let us note that the set $\{cos(\frac{\pi kx}{A})\, cos(\frac{\pi ly}{A}); k, l \in \mathbb{N} \cup \{0\}\}$ forms a complete orthogonal basis of the space $L^2(\Omega)$ and each of the functions satisfies no-flux boundary condition in agreement with (1.7) (see also [2]), so they are good to approximate the solutions to system (1.4)-(1.5). Inserting

$$\mathbf{u} = e^{\lambda_{k,l}t}\,\mathbf{W}(\mathbf{r})$$

into system (3.3) we obtain the algebraic system:

$$\lambda_{k,l}\mathbf{W} = -\mathbf{D}\mathbf{z}^2\mathbf{W} + \mathbf{B}\mathbf{W} \tag{3.7}$$

where we have defined

$$\mathbf{z} := \sqrt{\frac{\pi^2}{A^2}}\,(k,l)^T := \sqrt{w}\,(k,l)^T. \tag{3.8}$$

In view of (3.7), two things should be noticed. First, according to this equality, we can interpret $\mathbf{W}$ as the *eigenfunction* of the linearization of the *stationary* counterpart of system (1.4)-(1.5) corresponding to the *eigenvalue* $\lambda_{k,l}$ of the matrix

$$\mathbf{M} := \mathbf{B} - \mathbf{D}\mathbf{z}^2. \tag{3.9}$$

Thus, $\lambda_{k,l}$ is a solution to the equation:

$$\det \begin{bmatrix} -z^2 D\Gamma(\phi_0) - \lambda & z^2\chi_0\phi_0 \\ a & -\gamma - z^2 D_c - \lambda \end{bmatrix} = 0 \tag{3.10}$$

where $z^2 = \mathbf{z}^2$. Consequently, we obtain

$$\lambda_{\pm\, k,l} =: \lambda_\pm(z^2) = \frac{1}{2}\{-b \pm \sqrt{b^2 - 4z^2 c}\} \tag{3.11}$$

where

$$\begin{aligned} b &= \gamma + (D\Gamma(\phi_0) + D_c)z^2, \\ c &= \gamma D\Gamma(\phi_0) + DD_c\Gamma(\phi_0)z^2 - a\chi_0\phi_0. \end{aligned} \tag{3.12}$$

It is easy to note that, independently of $z^2 \geq 0$, the right hand side of (3.11) is real for positive values of the parameters appearing in Eq.(3.10). It is also seen from the above expressions that the '$-$' branch is strictly negative if $\gamma > 0$. Next, given the other parameters, the '$+$' branch can contain eigenvalues with positive real part if only $c < 0$ for some values of z^2, i.e. if the chemotaxis parameter χ_0 is sufficiently large. Moreover, the eigenvalues with positive real part are real. Thus, $\lambda_+(z^2) > 0$ if and only if

$$z^2 \in \Big(0, \frac{a\chi_0\phi_0 - \gamma D\Gamma(\phi_0)}{DD_c\Gamma(\phi_0)}\Big) \tag{3.13}$$

which, due to (1.9), is equivalent to

$$z^2 \in \Big(0, \frac{\tilde{a}\mu\beta\phi_0 - \gamma\Gamma(\phi_0)}{D_c\Gamma(\phi_0)}\Big). \tag{3.14}$$

Consequently, because the smallest positive value of z^2 is equal to w, the above condition implies that there exists at least one positive eigenvalue, if

$$\chi_0 > \frac{D\Gamma(\phi_0)(\gamma + D_c w)}{a\phi_0}$$

which, due to (1.6) and (1.9), can be written as

$$\mu > \frac{\Gamma(\phi_0)(\gamma + D_c w)}{aL_x^{(0)} L_y^{(0)} \beta\phi_0} = \frac{\Gamma(\phi_0)(\gamma + D_c w)}{\tilde{a}\beta\phi_0}. \tag{3.15}$$

The above relations are illustrated in Figure 1. It is shown there for the set of parameters given by (3.18), the '+' branch of eigenvalues comprises positive values (right panel), whereas if $\mu = 0.005$ (instead of $\mu = 0.1$), the two branches of eigenvalues are negative (left panel). The value of the right hand side of inequality (3.15) approximately equals to 0.0072.

Having the eigenvalues $\lambda_\pm(z^2)$, we can calculate the corresponding eigenvectors of $\mathbf{M}$:

$$\mathbf{E} = \mathbf{E}(\lambda_{\pm\, k,l}) = \mathbf{E}(\lambda_\pm(z^2)) := \mathbf{E}_\pm(z^2).$$

It can be checked that we can normalize the eigenvectors by supposing that $E_{\pm\, 1}(z^2) = 1$. Suppose that at time $t = 0$ we change the constant steady state by a spatially non-uniform perturbation $\omega(\mathbf{r})$. One can expect that, at least for some choices of $\omega(\mathbf{r})$ the constant steady state may evolve to a solution exhibiting features of a spatial pattern. It is obvious that, *locally in time*, this may be the case, if the expansion of the function ω on the basis of eigenfunctions of the linearized system contains non-zero contribution from the eigenfunctions assigned to positive eigenvalues of this system. To be more precise, let

$$\omega(\mathbf{r}) = \begin{pmatrix} \omega_\phi(\mathbf{r}) \\ \omega_c(\mathbf{r}) \end{pmatrix} \cong \sum_{(k,l)\in\mathcal{M}_+} c_{+\,k,l}\mathbf{W}_{+\,k,l}(\mathbf{r}) + \sum_{(k,l)\in\mathcal{M}_-} c_{-\,k,l}\mathbf{W}_{-\,k,l}(\mathbf{r}) \tag{3.16}$$

where

$$\mathbf{W}_{\pm\,k,l}(\mathbf{r}) := \mathbf{E}_\pm(z^2)\, cos(\frac{\pi kx}{A})\, cos(\frac{\pi ly}{A}),$$

and $\mathcal{M}_\pm$ are given sets of pairs (k,l) such that $k,l \in \mathbb{N} \cap \{0\}$ and $(k,l) \neq (0,0)$. We thus assume that if

$$U := \{(k,l) : \lambda_{+\,k,l} > 0\},$$

and

$$\mathcal{C} := \{(k,l) : c_{k,l} \neq 0\},$$

then

$$U \cap \mathcal{C} \neq \emptyset.$$

In (3.16) we assume that the right hand side converges in an appropriate norm. To simplify the problem of convergence we will assume that

$$\mathcal{M}_+, \mathcal{M}_- \quad \text{are finite sets.}$$

Such a cut off may be justified biologically by the nonzero size of the cells. As it is seen, in (3.16) we do not take into account the eigenvector corresponding to $\lambda = 0$, because this would be equivalent just to changing the constant spatially uniform state of the (linearized) system. The evolution of the initial data in (3.16) is given by the formula:

$$\begin{pmatrix} \phi(\mathbf{r},t) \\ \\ c(\mathbf{r},t) \end{pmatrix} \cong \begin{pmatrix} \phi_0 \\ \\ c_0 \end{pmatrix} + \tag{3.17}$$

$$\sum_{(k,l)\in\mathcal{M}_+} c_{+\,k,l} e^{\lambda_{+\,k,l}\,t}\ \mathbf{W}_{+\,k,l}(\mathbf{r}) + \sum_{(k,l)\in\mathcal{M}_-} c_{-\,k,l} e^{\lambda_{-\,k,l}\,t}\ \mathbf{W}_{-\,k,l}(\mathbf{r}).$$

Of course, the pattern may be transient as a solution to the nonlinear system (1.4)-(1.5), i.e. it may exist for some time and then disappear, or it may be unstable. However, here we are not interested in the asymptotic in time behaviour of this local in time pattern. The justification of such an approach may be of a heuristic type. Thus, many biological systems pass through the weakly nonstable states (patterns), which give rise to another kind of phenomenon (not taken into account in the considered model). It seems that the vasculogenesis process is just such a phenomenon: after the formation of the preliminary pattern of endothelial precursor cells, other interactions come into being (e.g. mechanical ones), which stabilize the obtained structure.

Here, we present the result of the above sketched method of calculations for the values of parameters chosen in the reference [14]. To be more precise we refer to Figure 6 in this paper. The parameters are taken as follows:

$$\begin{aligned} &D = 1/16,\ A = 100,\ \tilde{a} = 3.0,\ L_x^0 = L_y^0 := L^0 = 0.6 - 0.002/1.5, \\ &\beta = 15,\ \mu = 0.1,\ D_c = 0.5,\ \phi_0 = 0.54,\ \gamma = 0.014. \end{aligned} \tag{3.18}$$

Hence, due to (1.9) we have $\chi_0 = 0.0336$. The value of $\phi_0 = 0.54$ is implied by the fact that in Figure 6 in [14], 15000 cells were considered. The average volume of each of the cells is equal to $0.6^2 = 0.36$. As we assume that the cells are uniformly distributed inside the considered region, we conclude that the local volume fraction occupied by cells is equal to $1500 * 0.36/100^2 = 0.54$. Next, it is assumed that this steady state has been perturbed by 5%. The condition has been used in our simulations. As a result, for $t = 60$, we obtain a spatial distribution of volume fraction of cells coinciding with the distribution presented in Figure 6 in [14]. It is worthwhile to notice that, contrary to our symbolic approach, Figure 6 in [14] has been obtained by strictly numerical simulations. Next, in recovering transient structures, it is very important to take into account the whole set of eigenfunctions corresponding to both positive and negative eigenvalues of the linearized problem (3.1)-(3.2), because for small times all of these functions may play a significant role in pattern formation.

Apart from appropriate ratio of diffusion coefficients, it seems that the main problem in applying the Turing instability methodology to biological models, is to choose properly the perturbation of the initial spatially homogeneous state of the system. We are interested *first of all* in the time evolution of cell density, which is crucial from the point of view of the developing embryo. We thus perturb the system from its spatially homogeneous state (ϕ_0, c_0) by a nonuniform perturbation of the cell density $\omega(x, y)$. To guarantee the sufficient randomness of this perturbation we divide the spatial region $\Omega = \{(x, y) : x \in (0, A), y \in (0, A)\}$ into smaller 100^2 squares S_{ij}, $1 \leq i, j \leq 100$, with sides parallel to x and y axes of length equal to 1. For each of these squares we choose a random number r_{ij} from the interval $[-1, 1]$ and define ω_ϕ as a piecewise continuous function

$$\omega_\phi(x, y) = w\, r_{ij} H(S_{ij}) \tag{3.19}$$

where $H(S_{ij})$ denotes the characteristic function of the square S_{ij} and w is an appropriate scaling coefficient determining the magnitude of the perturbation. The same procedure can be applied to define the function $\omega_c(x, y)$.

To calculate the Fourier expansion coefficients, first let us note that

$$\int_0^A \int_0^A \Big[cos(\frac{\pi k_1 x}{A})\, cos(\frac{\pi l_1 y}{A})\Big]\Big[cos(\frac{\pi k_2 x}{A})\, cos(\frac{\pi l_2 y}{A})\Big] dxdy = \delta_{k_1 k_2}\delta_{l_1 l_2}\frac{A^2}{4}. \tag{3.20}$$

Due to the assumed normalization of the eigenvectors $\mathbf{E}_\pm$, the normalized Fourier coefficients $c_{-\,k,l}$, $c_{+\,k,l}$ satisfy the system

$$c_{-\,k,l} + c_{+\,k,l} = \frac{4}{A^2}\int_0^A \int_0^A \omega_\phi(x, y) cos(\frac{\pi k x}{A})\, cos(\frac{\pi l y}{A}) dxdy, \tag{3.21}$$

$$c_{-\,k,l} E_{-2}(z^2) + c_{+\,k,l} E_{+2}(z^2) = \frac{4}{A^2}\int_0^A \int_0^A \omega_c(x, y) cos(\frac{\pi k x}{A})\, cos(\frac{\pi l y}{A}) dxdy. \tag{3.22}$$

This system has always a unique solution $(c_{-\,k,l}, c_{+\,k,l})$, because the vectors $\mathbf{E}_-(z^2)$ and $\mathbf{E}_+(z^2)$ are linearly independent. In fact, $E_{-2}(z^2) < 0$ and $E_{+2}(z^2) > 0$.

Normalization and subtracting of the constant perturbation

To compare our approach with numerical simulations in [14], we take into account the fact that the initial spatially homogeneous stationary state was perturbed randomly by 5% (as it is stated in [14]). By adding a random number from the interval $[0, 1]$, we, on average, perturb the constant steady state ϕ_0 by $\pm$ 0.5, so to perturb it by 5% in every square S_{ij}, we must take $w = 0.05 \cdot \phi_0 \cdot 0.5^{-1} = 0.1\phi_0$ (see (3.19)). Finally, as is said above, in our approach we do not take into account the constant component of the perturbation functions, so we exclude it from our numerical code presented in Appendix B.

4. Transient Turing-like patterns on a sphere

In this section we will study the model of chemotaxis governed by system (1.4)-(1.5) on a sphere. Such a model may describe e.g., the onset of angiogenesis on the surface of a tumour volume or behaviour of receptors on the cell membrane, and in the context of Turing bifurcation their local aggregation. In the coordinates (θ, η) and with r being the radius of the sphere, the system governing the evolution of $\phi(\theta, \eta, t)$ and $c(\theta, \eta, t)$ has the following form

$$\begin{aligned}\frac{\partial \phi}{\partial t} = &\frac{D}{r^2 \sin\theta}\frac{\partial}{\partial \theta}\left(\sin(\theta)\Gamma(\phi)\frac{\partial \phi}{\partial \theta}\right) + \frac{D}{r^2 \sin\theta}\frac{\partial}{\partial \eta}\left(\Gamma(\phi)\frac{\partial \phi}{\partial \eta}\right)\\ &+\frac{\chi_0}{r^2 \sin\theta}\frac{\partial}{\partial \theta}\left(\sin(\theta)\phi\frac{\partial c}{\partial \theta}\right) + \frac{\chi_0}{r^2 \sin\theta}\frac{\partial}{\partial \eta}\left(\phi\frac{\partial c}{\partial \eta}\right),\end{aligned} \tag{4.1}$$

$$\frac{\partial c}{\partial t} = \frac{D_c}{r^2 \sin\theta}\frac{\partial}{\partial \theta}\left(\sin(\theta)\frac{\partial c}{\partial \theta}\right) + \frac{D_c}{r^2 \sin\theta}\frac{\partial^2 c}{\partial \eta^2} + a\phi - \gamma c. \tag{4.2}$$

Linearizing system (1.4)-(1.5) around a spatially homogeneous steady state $(\phi_0, c_0) = (\phi_0, \frac{\gamma}{a}\phi_0)$, we arrive at the following system:

$$\frac{\partial \phi}{\partial t} = \frac{D}{r^2}\Gamma(\phi)\Delta_S\phi - \frac{\chi_0\phi_0}{r^2}\phi\Delta_B c, \tag{4.3}$$

$$\frac{\partial c}{\partial t} = \frac{D_c}{r^2}\Delta_S c + a\phi - \gamma c \tag{4.4}$$

where Δ_S is the Laplace-Beltrami operator on the unit sphere (i.e. for $r = 1$):

$$\Delta_S := \frac{1}{\sin\theta}\frac{\partial}{\partial \theta}\left(\sin(\theta)\frac{\partial}{\partial \theta}\right) + \frac{1}{\sin\theta}\frac{\partial^2}{\partial \eta^2}.$$

Let us recall the real eigenfunctions of this operator. These are so called real spherical harmonics denoted by Y_{Lm}, where L is a nonnegative integer and $m \in \{-L, \ldots, 0, \ldots, L\}$. For fixed L, the functions Y_{Lm}, $m \in \{-L, \ldots, 0, \ldots, L\}$, span the $(2L+1)$-dimensional subspace of eigenfunctions corresponding to the eigenvalue $(-L(L+1))$, i.e.

$$\Delta_S Y_{Lm}(\theta, \eta) = -L(L+1)Y_{Lm}(\theta, \eta). \tag{4.5}$$

Every function Y_{Lm} is an appropriate linear combination of the standard (complex) functions Y_L^m and $Y_L^{(-m)}$. It can be assumed that, under proper normalization, the orthonormality condition is satisfied:

$$\int_0^{\pi}\int_0^{2\pi} Y_{L_1 m_1}(\theta, \eta)Y_{L_2 m_2}(\theta, \eta)\sin\theta \; d\eta \; d\theta = \delta_{L_1 L_2}\delta_{m_1 m_2}.$$

Similarly to the planar case, let

$$\mathbf{W}_{\pm\, Lm}(\theta,\eta) := \mathbf{E}_{\pm\, Lm} Y_{Lm}(\theta,\eta) \tag{4.6}$$

where $\mathbf{E}_{\pm\, Lm} \in \mathbb{R}^2$ are to be determined by demanding that $\mathbf{W}_{\pm\, Lm}(\theta,\eta)$ constitute eigenfunctions of the linearization of the stationary counterpart of system (4.3)-(4.4). We are looking for solutions to system (4.3)-(4.4) in the following form:

$$\begin{pmatrix} \phi(\theta,\eta,t) \\ c(\theta,\eta,t) \end{pmatrix} = \sum_{(L,m)\in\mathcal{M}_+} c_{+L,m} e^{\lambda_{+Lm} t}\, \mathbf{W}_{+Lm}(\theta,\eta) + \sum_{(L,m)\in\mathcal{M}_-} c_{-L,m} e^{\lambda_{-Lm} t}\, \mathbf{W}_{-Lm}(\theta,\eta). \tag{4.7}$$

As in the planar case, λ_{+Lm} and λ_{-Lm} denote the eigenvalues corresponding to the eigenvectors $\mathbf{E}_{+\, Lm}$ and $\mathbf{E}_{-\, Lm}$ of the matrix $\mathbf{M}$ defined below (see (4.8)). Thus putting the right hand side of (4.6) into (4.3)-(4.4), we obtain by means of (4.5):

$$\lambda_{\pm Lm}\mathbf{E}_{\pm\, Lm} = -\mathbf{D}\frac{L(L+1)}{r^2}\mathbf{E}_{\pm\, Lm} + \mathbf{B}\mathbf{E}_{\pm\, Lm}$$

where the matrices $\mathbf{D}$ and $\mathbf{B}$ are defined in (3.4). It follows that if

$$\mathbf{M} := \mathbf{B} - \mathbf{D}\frac{L(L+1)}{r^2}, \tag{4.8}$$

then $\lambda_{\pm Lm}$ must satisfy the equation $\det(\mathbf{M} - \lambda\mathbf{I}) = 0$, i.e.

$$\det\begin{bmatrix} -\dfrac{L(L+1)}{r^2}D\Gamma(\phi_0) - \lambda & \dfrac{L(L+1)}{r^2}\chi_0\phi_0 \\ a & -\gamma - \dfrac{L(L+1)}{r^2}D_c - \lambda \end{bmatrix} = 0. \tag{4.9}$$

Having the eigenvalues $\lambda_{\pm Lm}$ of the matrix $\mathbf{M}$, we are able to find the corresponding eigenvectors $\mathbf{E}_{\pm Lm}$. Let us note that the eigenvalues $\lambda_{\pm Lm}$ (as well as the eigenvectors $\mathbf{E}_{\pm Lm}$) depend, in fact, only on the integer L. Thus

$$\lambda_{\pm L(-L)} = \lambda_{\pm L(-L+1)} = \ldots = \lambda_{\pm L(L-1)} = \lambda_{\pm LL} =: \lambda_{\pm L}.$$

Moreover, if the volume fraction ϕ_0 in both of the analyzed cases is the same, then by identifying $\dfrac{L(L+1)}{r^2}$ with z^2, we can repeat the analysis of the planar case. To be more precise, if the units of length are given by the equality

$$\frac{L(L+1)}{r^2} \cong \frac{\pi^2}{A^2}(k^2+l^2), \tag{4.10}$$

then we have the approximate correspondence $\lambda_{\pm L} \cong \lambda_{\pm k,l}$.

It is obvious that the dominating spatial frequency in the transient patterns should depend both on the area of the sphere as well as on the number and size of the cells living on its surface. On one hand, due to (4.10), it follows from the analysis of the planar case that the number of possible positive eigenvalues increase with r^2 (because in the planar case the eigenvalues depend only on z^2). On the other hand, from the biological point of view, the spatial frequency of the initial perturbation is bounded from above by the size of cells, because in a region having an area corresponding to the area of the average cell, we have either single cell or no cell.

Let us consider early stages of tumour angiogenesis. Suppose that the boundary of a ball-shaped tumour has an area equal to 2.8 cm^2. This implies that around 1500000 endothelial cells of the average area about 100 μm^2 occupying 0.54 volume fraction are distributed on the boundary of the tumour region. Assuming that the size of the cells in [14] corresponds to 0.6-1.2 μm, we can conclude that A^2 corresponds to the area of 100-400 μm^2. It follows from (4.10) that in this case the number of pattern maxima is at least 700 times bigger than in the case analyzed in [14], which, due to the right panel of Figure 1 (and Figure 6 in [14]) is a huge number. This proves that the considered angiogenetic structure can be extremely complicated. Let us also note that, if we assume that the presented model of chemotaxis holds also in this case, then, due to (3.14), the maximal value of $L(L+1)$ (equivalent to k^2+l^2 in the planar geometry) does not depend on D. This seems important in view of the fact that the motility of cells may be very low in some tissues.

Let us finally check, if we can use the above model, to consider the problem of receptor clusterization on the surface of immune B cells [11, 12]. In this case we should, however, adapt the assumptions concerning the volume fraction of the agglomerated objects, which are now receptor proteins. Let us consider the B cell as a ball of radius equal to 6μm. Suppose that the number of B cells receptors (BCRs) on its membrane is of the order of 10^5 [17]. Suppose further that the area occupied by a single BCR on the membrane (corresponding to more or less to the cross sectional area of BCR proteins) equals approximately 100 nm^2 := $(L^0\,\mu m)^2$. It follows that the volume fraction is approximately equal to $\phi_0 = 10^5 \cdot 10^2\ (4\pi \cdot 36 \cdot 10^6)^{-1} = 0.022$. Hence $\Gamma(\phi_0) \approx 1.14$. To obtain reasonable number of receptor clusters, we will use the following set of parameters:

$$\begin{aligned} &D = 1/16,\ r = 6,\ \tilde{a} = 3.0,\ L^0 = 10 \cdot 10^{-3}, \\ &\beta = 15,\ \mu = 0.1 \cdot 200,\ D_c = 0.1,\ \phi_0 = 0.022,\ \gamma = 0.014. \end{aligned} \tag{4.11}$$

The changes with respect to the set (3.18), are implied by the geometry (the values of r^{-2} corresponding to π^2/A^2, L^0 corresponding to the linear size of the objects), as well as by biochemical assumptions. To be more precise, we decreased the value of D_c to $0.1\mu m^2/s$, because the diffusion of proteins on the membrane is extremely small, and increased 200 times the absolute value of the effective chemical potential μ. We should keep in mind that the last change may not have a straightforward biological interpretation and has been introduced 'ad hoc' to compensate the decrease of the volume fraction ϕ_0 with respect to the planar case.

For the above set of parameters, according to inequality (3.14), we obtain the maximal value of $L(L+1)$ for which $\lambda_{+L} > 0$ to be equal approximately to 6230 and the value of $L(L+1)$ corresponding to the largest λ_{+L} to be equal to 1600 (see, the right panel of Figure 3). So,

in principle, we can obtain over 6000 receptor clusters. This is in a qualitative agreement with the references [7, 8, 16], where clusters of 10-20 receptors were considered as characteristic active 'quants' of receptors capable to activate stably a B cell.

The process of receptors clustering is often more complicated and may be also connected with some external factors. For example, the B cell clusters can be formed by receptor cross-linking due to binding of polyvalent ligands recruited from the solution [4]. Similarly, the receptor clusters can be formed by a B cell contact with an antigen-presenting cell (APC) loaded with antigens. In this case even monovalent ligands are also capable to initiate BCR signaling if presented on APC [3,15]. Nonetheless, it seems that the diffusion of receptors together with their tendency to aggregate due to some attractive interactions mediated by other agents, is the main ingredient in the process of their pattern formation. On the other hand, even if the receptors are completely immobile, they can create active regions via their interaction with cytosolic kinase molecules. Such a model was studied in [11, 12]. In principle, a similar method can be used to study the formation of Turing patterns in this volume-surface case.

5. Conclusions

In the paper, we studied the behaviour of solutions to the system partial differential equations derived in [14] and obtained by taking the macroscopic limits in a stochastic model taking into account cell diffusion and cell-cell interaction mediated by auxiliary molecules. The model is dedicated principally to description of bacterial structures formed due to chemotactic attraction, but its generality allows us to extend its validity to other cellular phenomena consisting in spatial pattern formation. Such processes play crucial role in cellular biology. On one hand, they are a background of morphogenesis, on the other hand they may be an onset, e.g. of angiogenesis leading to creation of an alimentary system of cancer cell population. Our approach is in the spirit of the Turing bifurcation theory, but specifically we concentrated on transient spatial structures. Such structures exist for some time, but may be not stable from the mathematical point of view. However, biologically, such structures can be stabilized by some other factors, which are not considered explicitly in the mathematical model. To track the formation of transient patterns, we considered the expansion of initial perturbation into eigenfunctions corresponding both to positive, as well as negative eigenvalues of the linearized system. The patterns obtained by the above procedure are very similar to the spatial patterns obtained in [14] via numerical simulations. Due to the large number of eigenfunctions used in the expansion of the solution, we used the Mathematica package to carry out the calculations. Using analogous analysis we considered the same system of equations, but in the spherical geometry. In this way we can describe spatial patterns on the boundary of cells or boundaries of various three dimensional multi-cellular structures. In the paper, we studied the formation of angiogenetic network of a ball-shaped tumour. In Appendix B we provide a Mathematica code used in the analysis of spatial patterns in the planar case.

Appendix

A. Figures

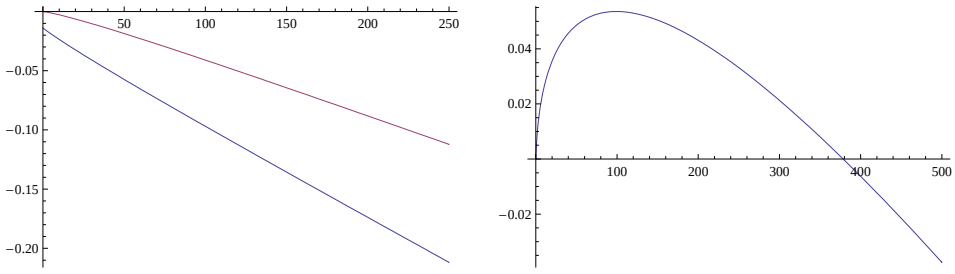

FIGURE 1. Left panel: The two branches of eigenvalues as a function of (k^2+l^2) for $\mu = 0.005$ and other parameters as in (3.18). Both of the branches are negative for $(k^2+l^2) > 0$. Right panel: The '+' branch of eigenvalues as a function of (k^2+l^2) for all the parameters as in (3.18) (in particular $\mu = 0.1$).

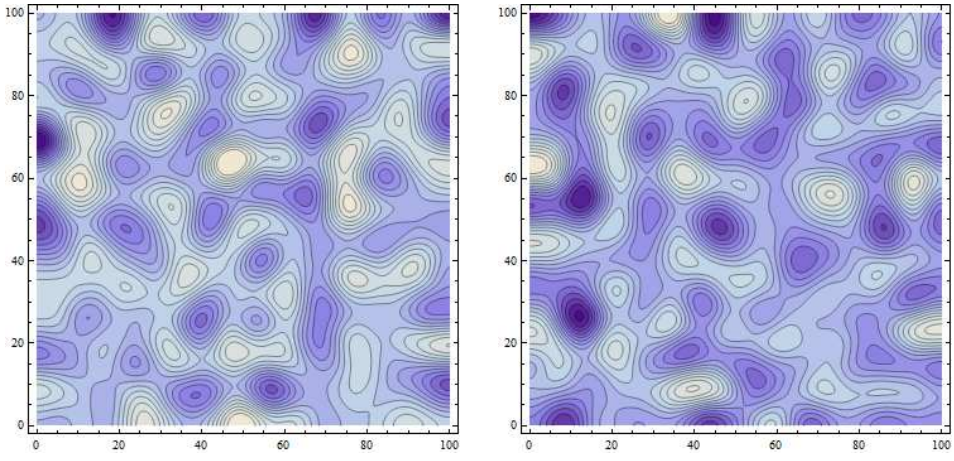

FIGURE 2. Early vascular network formation at $t = 60$ obtained via the Mathematica code presented in the Appendix. The lightest colour corresponds to $\phi \cong 0.7$ and the darkest to $\phi \cong 0.4$. Left and right panel: the flat colour map corresponding to Figure 6 in [14] for two different stochastic perturbation described in the text.

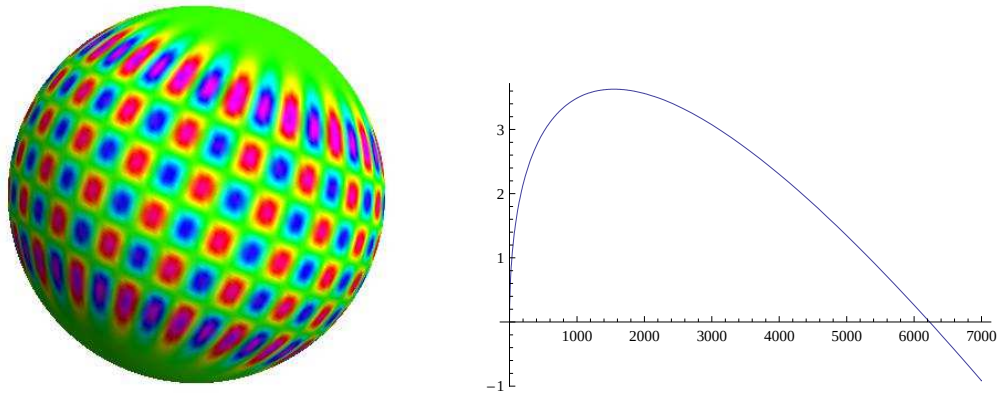

FIGURE 3. Left panel: A graphical presentation of the function Y_{Lm} with $L = 24$ and $m = 19$. Right panel: The '+' branch of eigenvalues $\lambda_{+Lm} = \lambda_{+L}$ as a function of $L(L+1)$ for all the parameters as in (4.11) (in particular $\mu = 0.1 \cdot 200$).

B. Mathematica code

Here we insert a Mathematica code with commands realizing the successive steps of the procedure leading to obtain Figure 2. The procedure is described in section 3.

We will make the following change of denotations:

$$D \to d,\ D_c \to S,\ L^0 \to L,\ \tilde{a} \to a,\ \chi_0 \to h,\ \beta \to b,\ \phi_0 \to u,\ \gamma \to gamma,\ \mu \to m,$$
$$\lambda_- \to W1,\ \lambda_+ \to W2,\ \mathbf{E}_- \to V1,\ \mathbf{E}_+ \to V2, c_{-\,k,l} \to \frac{4}{A^2} B1(k,l),\ c_{+\,k,l} \to \frac{4}{A^2} B2(k,l). \tag{A.1}$$

(* We read in the values of the parameters.*)

d = 1/16; G = d*(1+u)/(1-u+u*Log[u]); A = 100; w = Pi^2/A^2; a = 3.0; L = 0.6 - 0.002/1.5; S = 0.5; m = 0.1; b = 15; h = d*m*b*L^2; u = 0.54; gamma = 0.014;

(* We create a matrix MZ (see (3.9)), and compute its eigenvalues.*)

MZ = {{ - Z*G, Z*h*u }, {a/L^2, -gamma-S*Z }}; WZ = Eigenvalues[MZ]

(*We plot the real and imaginary parts of the first and second eigenvalues. *)

```
Plot[{Re[WZ[[1]]],Re[WZ[[2]]]},{Z,0,10}]
Plot[{Im[WZ[[1]]],Im[WZ[[2]]]},{Z,0,10}]
```

(* We create the matrix M with Z from the matrix MZ by replacing Z with $w(k^2 + l^2)$ and compute its eigenvalues.*)

M = {{ - w*(k^2+l^2)*G, w*(k^2+l^2)*h*u }, {a/L^2, -gamma-S*w*(k^2+l^2) }}; W = Eigenvalues[M]

(* We table the real parts of the second and first eigenvalues for different values of k and l, where $0 \leq k, l \leq 30$. This choice is dictated by the fact that for $k^2 + l^2 > 900$ the values of λ_+ are negative and relatively large in their absolute value (see right panel of Figure 1). *)

```
TW1 =Table[{{k,l},Re[W[[1]]]},{k,0,30},{l,0,30}];
TW2 =Table[{{k,l},Re[W[[2]]]},{k,0,30},{l,0,30}];
```

(* We calculate the eigenvectors $V1(k^2 + l^2)$ corresponding to the eigenvalues $W1(k^2 + l^2)$, and the eigenvectors $V2(k^2 + l^2)$ corresponding to the eigenvalues $W2(k^2 + l^2)$ (confer (A.1)). In defining the eigenvectors corresponding to the eigenvalue $W1$ we resign from the normalization condition $V1_1 = 1$ and replace them by the vectors {0,1}, every time their second component exceeds 10^{12}. *)

TV1 = Table[If [Abs[a/L^2/(gamma + w*(k^2 + l^2) S + W[[1]])] > 10^12, {{k, l}, {0, 1}}, {{k, l}, {1, a/L^2/(gamma + w*(k^2 + l^2) S + W[[1]])}}], {k, 0, 30}, {l, 0, 30}];

TV2 = Table[{{k, l}, {1, a/L^2/(gamma + w*(k^2 + l^2) S + W[[2]])}}, {k, 0, 30}, {l, 0, 30}];

(* We define the piecewise continuous unnormalized function $\omega_\phi(x, y) : A \times A \to \mathbb{R}$ by choosing randomly real numbers within the range $\{-1, 1\}$ in the small unit squares corresponding to i, j, where $0 \leq i, j \leq 99$. *)

```
TFR=Table[{{i,j}, Random[Real,{-1,1}]},{i,0,99},{j,0,99}];
```

(* Likewise, we define the piecewise continuous unnormalized function $\omega_c(x, y) : A \times A \to \mathbb{R}$. *)

```
TCR=Table[{{i,j}, Random[Real,{-1,1}]},{i,0,99},{j,0,99}];
```

(* We calculate the coefficients of expansion of the initial data $\omega_\phi(x, y)$ in the basis of functions $cos(\frac{\pi kx}{A})\, cos(\frac{\pi ly}{A})$ by computing approximate values of the integrals on the right hand sides of (3.21) and (3.22). *)

```
TF=Table[{{k,l},Sum[TFR[[i]][[j]][[2]]*Cos[0.5+TFR[[i]][[j]][[1]]
[[1]]*Pi*k/100]*Cos[0.5+T[[i]][[j]][[1]][[2]]*Pi*l/100],
{i,1,100},{j,1,100}]},{k,0,30},{l,0,30}];


TC=Table[{{k,l},Sum[TCR[[i]][[j]][[2]]*Cos[0.5+T[[i]][[j]][[1]]
[[1]]*Pi*k/100]*Cos[0.5+TCR[[i]][[j]][[1]][[2]]*Pi*l/100],
{i,1,100},{j,1,100}]},{k,0,30},{l,0,30}];
```

(* We solve system (3.21)-(3.22) to calculate the coefficients B1 and B2 determining the coefficients $c_{-\,k,l}$ and $c_{+\,k,l}$ (see (A.1). *)

```
TCoeff = Table[{{k,l},
B1 = B1H/.{Solve[{TF[[k]][[l]][[2]],TC[[k]][[l]][[2]]} = =
B1H*TV1[[k]][[l]][[2]] + B2H*TV2[[k]][[l]][[2]],{B1H,B2H}][[1]][[1]]},
B2 = B2H/.{Solve[{TF[[k]][[l]][[2]],TC[[k]][[l]][[2]]} = =
B1H *TV1[[k]][[l]][[2]] + B2H*TV2[[k]][[l]][[2]],{B1H,B2H}][[1]][[2]]}},
{k,1,31}, {l,1,31}];
```

(* We make the contour plot of the resulting pattern according to (3.17) and the remarks following (3.17) concerning the normalization and subtraction of the constant component. *)

```
FR =0.1*0.54*(50)^(-2)*(Sum[(TCoeff[[k]][[l]][[3]]*
Exp[60*TW2[[k]][[l]][[2]]] +
TCoeff[[k]][[l]][[2]]*Exp[60*TW1[[k]][[l]][[2]]])*
Cos[TF[[k]][[l]][[1]][[1]]*Pi x/100]*
Cos[TF[[k]][[l]][[1]][[2]]*Pi*y/100]*(1-1/2*KroneckerDelta[k,l]),
{k,1,31}, {l,1,31}]-
1/2*(TCoeff[[1]][[1]][[3]]*Exp[60*TW2[[1]][[1]][[2]]] +
TCoeff[[1]][[1]][[2]]*Exp[60*TW1[[1]][[1]][[2]]]));
%\end{lstlisting}

CP =ContourPlot[FR+0.54,{x,0,100},{y,0,100},PlotPoints->100,
PlotRange->All,ColorFunction->"LakeColors"]
```

Acknowledgements. This work was partially supported by grant NCN 2014/13/B/NZ2/03840.

References

[1] M. Alber, R. Gejji, B. Kazmierczak. *Existence of global solutions of a macro-scopic model of cellular motion in a chemotactic field*. Appl. Math. Lett., 22 (2009), 1645-1648.

[2] M. Alber, T. Glimm, H.G.E. Hentschel, B. Kazmierczak, S.A. Newman. *Stability of n-dimensional patterns in a generalized Turing system: implications for biological pattern formation*. Nonlinearity, 18 (2005), 125-138.

[3] F.D. Batista, D. Iber, M.S. Neuberger. *B cells acquire antigen from target cells after synapse formation*. Nature, 411 (2001), 489-494.

[4] R.J. Brezski, J.G. Monroe. *B-cell receptor*. Adv. Exp. Med. Biol., 640 (2008), 12-21.

[5] Y.R. Carrasco, F.D. Batista. *B cells acquire particulate antigen in a macrophage-rich area at the boundary between the follicle and the subcapsular sinus of the lymph node*. Immunity, 27 (2007), 160-171.

[6] S. Christley, M.S. Alber, S.A. Newman. *Patterns of mesenchymal condensation in a multiscale, discrete stochastic model*, PLoS Comput. Biol., 3 (2007), e76.

[7] H.M. Dintzis, R.Z. Dintzis, B. Vogelstein. *Molecular determinants of immunogenicity: the immunon model of immune response*. Proc. Natl. Acad. Sci. USA, 73 (1976), 3671-3675.

[8] R.Z. Dintzis, M.H. Middleton, H.M. Dintzis, *Studies on the immunogenicity and tolerogenicity of T-independent antigens*. J. Immunol., 131 (1983), 2196-2203.

[9] A. Gamba, D. Ambrosi, A. Coniglio, A. De Candia, S.Di Talia, E. Giraudo, G. Serini, L. Preziosi, F. Bussolino. *Percolation, morphogenesis, and Burgers dynamics in blood vessels formation*. Phys. Rev. Lett., 90 (2003), 118101.

[10] S. Guido, D. Ambrosi, E. Giraudo, A. Gamba, L. Preziosi, F. Bussolino. *Modeling the early stages of vascular network assembly*. EMBO J., 22 (2003), 1771-1779.

[11] B. Hat, B. Kazmierczak, T. Lipniacki. *B cell activation triggered by the formation of the small receptor cluster: a computational study*. PLoS Comput Biol, 7 (2011), e1002197.

[12] B. Kazmierczak, T. Lipniacki. *Regulation of kinase activity by diffusion and feedback*. J. Theor. Biol., 259 (2009), 291–296.

[13] R. Kowalczyk. *Preventing blow-up in a chemotaxis model*. J. Math. Anal. Appl., 305 (2005), 566-588.

[14] P.M. Lushnikov, N. Chen, M. Alber. *Macroscopic dynamics of biological cells interacting via chemotaxis and direct contact*. Phys. Rev. E, 78 (2008), 061904.

[15] P. Tolar, J. Hanna, P.D. Krueger, S.K. Pierce. *The constant region of the membrane immunoglobulin mediates B cell-receptor clustering and signaling in response to membrane antigens*. Immunity, 30 (2009), 44-55.

[16] B. Vogelstein, R.Z. Dintzis, H.M. Dintzis. *Specific cellular stimulation in the primary immune response: a quantized model*. Proc. Natl. Acad. Sci. USA, 79 (1982), 395-399.

[17] J. Yang, M. Reth. *Oligomeric organization of the B-cell antigen receptor on resting cells*. Nature, 467 (2010), 465-469.